JOURNAL OF Applied Polymer SCIENCE

Morphology of Polypropylene/Silica Nano- and Microcomposites

Anđela Pustak,[1] Irina Pucić,[1] Matjaž Denac,[2] Iztok Švab,[3] Janez Pohleven,[2] Vojko Musil,[2] Ivan Šmit[1]

[1]Ruđer Bošković Institute, Division of Materials Chemistry, Bijenička 54, 10002 Zagreb, Croatia
[2]FEB Maribor, Institute of Technology, University of Maribor, Razlagova 14, 2000 Maribor, Slovenia
[3]ISOKON, Production and Processing of Thermoplastics, Ltd, Mestni trg 5a, 3210 Slovenske Konjice, Slovenia
Correspondence to: I. Šmit (E-mail: ismit@irb.hr)

ABSTRACT: The aim of this study was to compare the effects of different silica grades on the structure and morphology of isotactic polypropylene (iPP)/silica composites to better understand their structure–property relationships. Isotactic polypropylene composites with 2, 4, 6, 8 vol % of added silica fillers differing in particle size (micro- vs. nanosilica) and surface modification (untreated vs. treated surface) were prepared by nonisothermal compression molding and characterized by different methods. The addition of all silica fillers grades to the iPP matrix significantly influenced the spherulitic morphology, while phase characteristics of the iPP matrix seemed to be unaffected. Surface modification of silica fillers exhibited stronger effects on spherulite size than size of silica particles. Nonpolar silica particles, more miscible or compatible with iPP chains than polar silica particles, enabled better spherulitic growth. The spherulite sizes tended to reach equal values at 8 vol % of added silicas showing that spherulite size became independent of filler concentration and surface modification above optimum filler concentration. © 2012 Wiley Periodicals, Inc. J. Appl. Polym. Sci. 000: 000–000, 2012

KEYWORDS: composites; morphology; polyolefins; structure–property relations

Received 27 January 2012; accepted 19 August 2012; published online
DOI: 10.1002/app.38487

INTRODUCTION

Among polyolefins polypropylene is one of the most widely used commodity plastomers because of its outstanding properties and versatile applications of its composites. Because of favorable cost/performance ratio, compounding of polymers with different fillers is the economic venue for shaping the desired properties and expanding the product range.[1–3] Common mineral fillers used in composites for modification of isotactic polypropylene (iPP) [0]are talc, calcium carbonate, glass beads and fibers, mica, silica, and wollastonite.[1–3] Fillers affect the ultimate mechanical properties in two ways: (i) by acting as reinforcement (effect of shape, size, and modulus)[4] and (ii) by affecting crystallization of polymer matrix (phase and supermolecular structure of semicrystalline polymer) and composite morphology.[5] Accordingly, important reinforcing effect is caused by the filler, while the structure and morphology of composites depend on particle–particle and particle–polymer interactions.[2–6]

Shaping of polymer composites optimal mechanical properties could be achieved by studying their structure–property relationships. In presented part of study the main focus is on the structure of the iPP/silica composites. Previously published studies of binary iPP/silica composites were mainly focused on two goals: preparation of new composite materials with improved mechanical properties[6–11] and phenomenological study of crystallization usually under nonisothermal conditions.[12–19] Improving of mechanical properties was mainly focused on reduction of silica particle agglomeration by nanoparticles surface treatment.[7–11] Early investigations of composites showed the decrease of spherulite size in polymer matrix caused by nucleation effect of fillers.[20] Crystallization studies of the iPP/silica composites comprised the investigations of nanosilica properties (size, surface properties, shape, and concentration) effects on nucleation and spherulite growth. Although the results on nanosilica effects concerning nucleation and crystallization rate complied to expectations of the investigators, the effects of surface modification of silica nanoparticles on the crystallization in the iPP matrix were controverisal.[11–15] Also, some authors pointed out to the effects of reduced diffuse chain mobility due to the presence of nanoparticles[15–17] and specific particle properties[18] on the crystallization behavior of composites.

Having in mind the complex correlation of the properties and content of various silica grades, systematic research of the structure/morphology–mechanical/adhesion property relationships of non-isothermally crystallized compression molded iPP/silica composites was performed. Such approach enables shaping of

Table I. Filler Characteristics

Samples	Trade name of filler	Tapped density (g L^{-1})	Surface modification	Specific surface area (BET) (m^2 g^{-1})	Average particle size, d_{50}
A-200	Aerosil 200; unmodified nanosilica	~ 50	none	200 ± 25	12 nm
A-R7200	Aerosil R7200; modified nanosilica	~ 230	methacryl-silane	150 ± 25	12 nm
A-R8200	Aerosil R8200; modified nanosilica	140	hexamethyl-disilazane	160 ± 25	12 nm
S-120	Sipernat 120; unmodified microsilica	185	none	125	14.5 μm
S-D17	Sipernat D17; modified microsilica	150	2% chem. bounded carbon	100	10 μm

composites properties or at least selecting of an appropriate silica filler to obtain optimal (mechanical) properties for a particular application.

This article relates to the structure and morphology of binary iPP/silica composites. Silica fillers used in this study differed in size (nano- *vs.* micro-) and surface properties (hydrophilic vs. hydrophobic, e.g., polar vs. nonpolar). Effects of fillers were investigated on the new special hydrophobic fumed nanosilica generation (Aerosil R7200 and Aerosil R8200) and compared with the parent hydrophilic Aerosil 200 nanosilica as well as precipitated hydrophobic Sipernat D17 with hydrophilic Sipernat 120 microsilicas. Mechanical properties and adhesion phenomena of the iPP/silica composites will be presented in the following paper.[19]

EXPERIMENTAL

Materials

The materials used in this study were isotactic polypropylene (iPP) and five types of silica fillers. The iPP used for sample preparation was Moplen HP501L, LyondellBasell Industries, Rotterdam, Netherlands (melt flow rate [MFR] (230°C/2.16 kg) = 6 g/10 min, $\rho = 0.90$ g cm^{-3}, $M_n = 120{,}000$ g mol^{-1}). Silica fillers were two proprietary microsilicas (unmodified Sipernat 120 and surface modified Sipernat D17) and three proprietary nanosilicas (unmodified Aerosil 200 and two surface modified nanosilicas Aerosil R7200 and Aerosil R8200); all silica grades were kindly supplied by Evonic Industries (Degussa), Essen, Germany. Filler characteristics are listed in Table I.

Sample Preparation

Binary iPP/silica composites with volume content ratios 100/0, 98/2, 96/4, 94/6, and 92/8 were prepared in an oil-heated Brabender kneading chamber. The components were put into a chamber preheated up to 200°C with a rotor speed of 50 min^{-1} and then kneaded for 7 min. After homogenization, the melt was rapidly transferred to a preheated laboratory press and compression molded into 1- and 4-mm-thick plates. The pressing temperature was 220°C, pressure 100 bar and the pressing time of 14 min for 1-mm and 11.5 min for 4-mm-thick plates. Afterward, the plates were cooled to room temperature in air.

Characterization

Wide-Angle X-Ray Diffraction (WAXD). Wide-angle X-ray diffraction (WAXD) was performed to determine possible effects of silica filler on some phase characteristics of the composites: phase structure, degree of crystallinity (evaluated by the Ruland method[21]), orientation (A_{110} and C parameters calculated by Zipper formulae[22]) and crystallite size. Wide-angle X-ray diffractograms of 1-mm-thick plates were taken with a Philips diffractometer PW 1820 diffractometer using monochromatized Cu Kα radiation in the diffraction range of $2\theta = 5$–40°.

Fourier Transform Infrared Spectroscopy. Samples of pure iPP and composites with iPP/silica content ratios 92/8 and 94/6 cut from 1-mm-thick compression molded plates were additionally pressed into thin films for infrared analysis. Fourier Transform Infrared Spectroscopy (FTIR) spectra of the samples were recorded on a Bruker Tensor 27 in the MID region (4000 to 400 cm^{-1}) and were processed using Bruker Opus software.

Differential Scanning Calorimetry. Thermal analysis was performed on a Perkin Elmer Diamond Differential Scanning Calorimetry (DSC). Samples (9.3–10.3 mg) were cut from 1-mm-thick compression molded plates, placed in aluminum pans and sealed. The instrument was calibrated using In and Zn according to the procedure defined by the manufacturer. Thermograms of the samples of pure iPP and composites with iPP/silica content ratios 92/8 and 94/6 were recorded in dynamic mode, at a heating rate of 5°C min^{-1} in an extra pure nitrogen environment. Two heating-cooling cycles were performed by first heating the sample from 50 to 200°C, keeping it at that temperature for 5 min and then cooling to 50°C at a cooling rate of 5°C min^{-1}.

Scanning Electron Microscopy. A SIRION 400 NC and Philips XL 30 scanning electron microscope (SEM) were used to study the morphology of composites. Samples were fractured in liquid nitrogen and covered with gold before being examined with a microscope at an acceleration voltage up to 10 kV at various magnifications. All SEM micrographs are secondary electron images.

Optical Microscopy (OM). A Leica light microscope (Model DMLS) coupled with a digital camera was used for observation of thin crossed microtomed sections (taken from 1-mm thick plates)

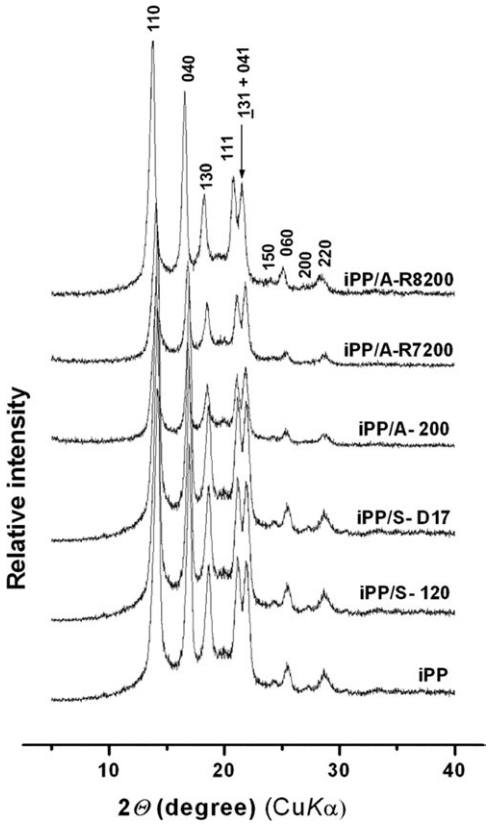

Figure 1. X-ray diffraction patterns of pure iPP and iPP/silica composites with 96/4 volume ratio (middle concentration range).

under crossed polarizers (POM) or phase contrast (PC). Maximal anisotropic diameter of spherulites ($d_{i,\max}$) was measured on several polarization micrographs of each sample and average spherulite diameter (d_{sph}) was calculated according to eq. (1):

$$d_{sph} = \frac{N_i d_{i,\max}}{N_i} \quad (1)$$

where N_i is the number of measured spherulites with the average diameter d_i.

RESULTS AND DISCUSSION

Phase Characteristics

X-ray diffraction (XRD) patterns of all pure silica powders (not shown) exhibit very similar diffraction curves with the main diffuse diffraction maxima at ~21.3° 2T for nanosilicas and at ~22.0° 2T for microsilicas, showing the amorphous character of all silica fillers. Small difference in peak position between nano- and microsilicas indicates somewhat higher average interplanar distances in disordered Si—O— networks of nanosilicas than microsilicas.

Diffraction curves of pure iPP and iPP/silica composites exhibit patterns of mainly monoclinic α-form of the iPP (Figure 1). Addition of a small amount of silica (2 vol %) negligibly changes half-maximum widths of the main diffraction peaks (110, 040, 130) of the α-iPP phase. Further addition of silica

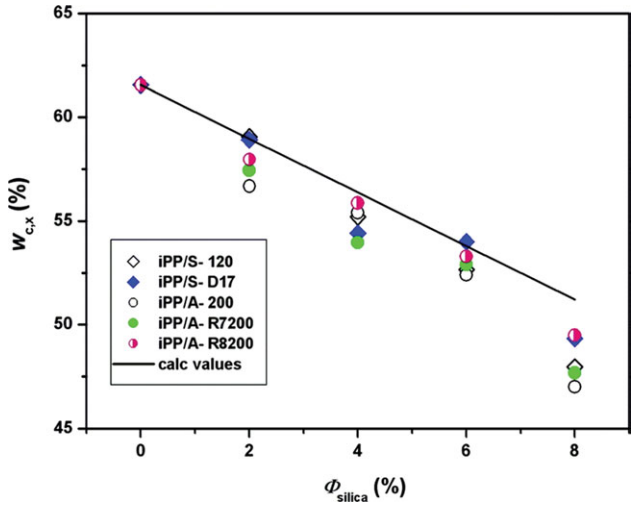

Figure 2. Degree of crystallinity of iPP/silica composites evaluated from X-ray diffractograms. [Color figure can be viewed in the online issue, which is available at wileyonlinelibrary.com.]

doesn't change the profile of any reflection. Obviously, the α-iPP crystallite size was not affected either by the type of silica filler or by the filler content. The values of orientation parameters A_{110} and C, calculated according to equations proposed by Zipper et al.,[22] also exhibit imperceptible changes with filler content (not shown).

Incorporation of amorphous silicas into the iPP matrix increases the intensity of the amorphous diffraction maximum, thus reflecting the increase in overall amorphous content (amorphous iPP phase + amorphous silica). The decrease in

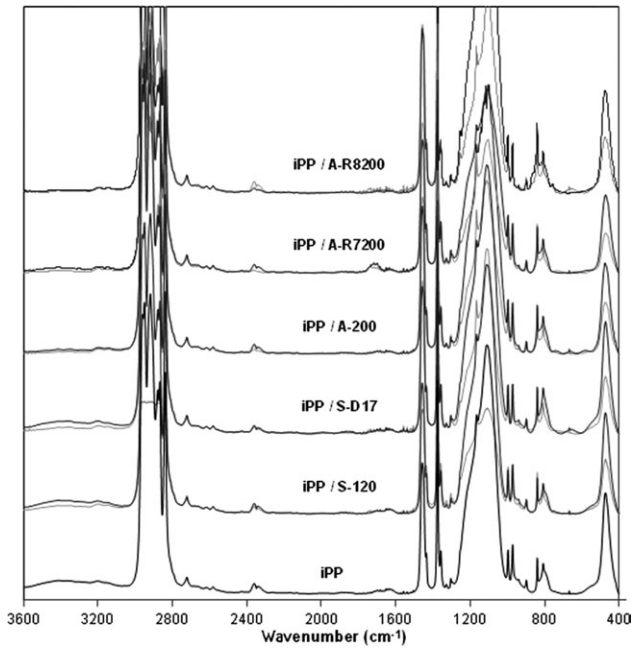

Figure 3. FTIR spectra of iPP (bottom black line) and iPP/silica composites with micro- and nanosilica fillers in volume ratios 92/8 (dark lines) and 94/6 (light lines).

Applied Polymer SCIENCE

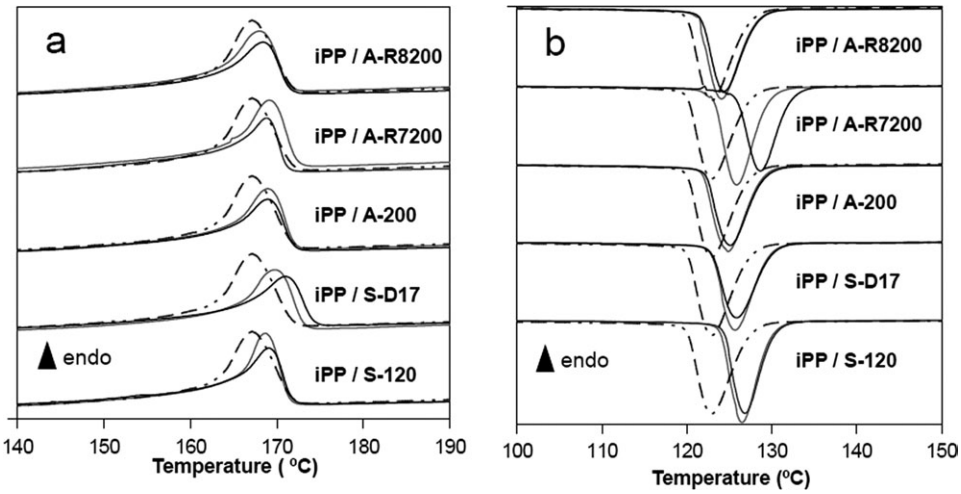

Figure 4. DSC scans of (a) second heating and (b) first cooling runs. Thermograms of neat iPP (dash dot line) and iPP/silica composites with volume content ratios 96/4 (gray lines) and 92/8 (black lines) are shown.

the degree of crystallinity, $w_{c,x}$, depended almost linearly on the content of silica in the samples (Figure 2). Theoretical crystallinity values of iPP, $w_{c,x}$, recalculated to the iPP fraction in composites, are presented by line in Figure 2. Experimental crystallinity values that are mainly below the theoretical ones are within the method resolution. The highest decrease in crystallinity and deviation from linearity were observed in all samples with the highest silica amount (8 vol %).

FTIR spectra were recorded to determine changes due to incorporation of micro- and nanosilica fillers to iPP. According to Painter et al.[23] the changes of absorptions at 1498, 1376, 1167, and 998 cm^{-1} could be related to crystallinity of iPP. In the spectra of samples containing silica relative intensities of these absorption bands were changed but no shifts were observed (Figure 3). The —Si—O—Si— bending absorption at 1100 cm^{-1} was one of the strongest absorptions in the spectra of all iPP-silica composites. The iPP peak at 1167 cm^{-1} appears as a shoulder on the strong Si—O absorption and the iPP absorption at 998 cm^{-1} is very close to the same silica absorption. Other relevant silica absorptions are wide peak at 810 cm^{-1} of medium intensity and stronger and sharper absorption at 470 cm^{-1}, both caused by —Si—O— stretching vibrations.[24] Low intensity wide absorption centered around 3400 cm^{-1} corresponds to the —OH groups. In samples with A-R7200, a small peak is present at 1720 cm^{-1} which originates from C=O groups in the methacrylsilane layer.[24]

Normalized DSC curves of the first cooling and the second heating runs of composite samples containing 4 and 8 vol % of each type of silica fillers are shown in Figure 4. Concentrations of 4 and 8% of filler were selected as the most representative and the corresponding data are listed in Table II. Addition of silica [4 vol %—grey lines and 8 vol %—black lines in Figure 4(a)] to the iPP (dash dot line) caused a relative widening of melting peaks, which is most pronounced for composites containing hydrophobic S-D17 microsilica. The peak temperature of melting in the iPP/silica composites, T_m, shifted to higher values with increased filler content. The end temperature remained unchanged except in samples containing S-D17 and

Table II. Crystallization and Melting Data for iPP and iPP/Silica Composites

		First crystallization cycle		Second melting cycle		
Compound	Composition	T_c (°C)	ΔH (J g^{-1})	T_m (°C)	ΔH (J g^{-1})	$\Delta T = T_m - T_c$
iPP	100/0	122.95	−100.78	167.12	94.70	44.17
S-120	92/8	126.85	−80.78	169.02	81.49	42.17
	96/4	126.51	−89.83	168.61	87.03	42.10
S-D17	92/8	125.88	−81.83	170.99	77.51	45.11
	96/4	125.66	−89.70	169.76	83.98	44.10
A-200	92/8	125.11	−82.08	168.97	77.30	43.86
	96/4	124.86	−91.31	168.94	85.53	44.08
A-R7200	92/8	128.65	−83.78	168.80	80.86	40.15
	96/4	125.88	−96.39	169.14	89.82	43.26
A-R8200	92/8	124.36	−83.78	168.38	77.05	44.02
	96/4	124.09	−96.39	167.96	85.04	43.87

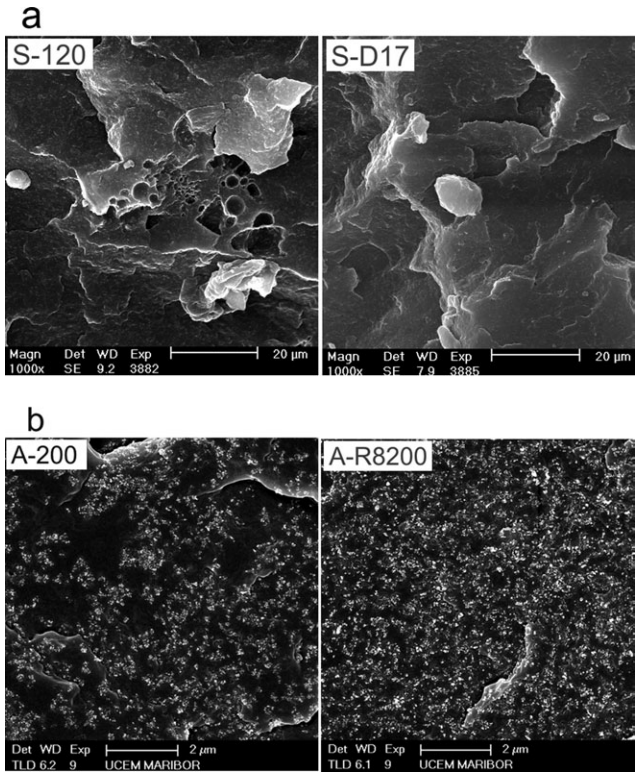

Figure 5. SEM micrographs of the iPP/silica 92/8 composites with (a) microsilicas S-120 and S-D17 and (b) nanosilicas A-200 and A-R8200.

A-R7200 fillers. Both melting and crystallization heats have lower values in composites compared to pure iPP.

Crystallization temperatures in the first and the second cooling cycles, T_c, also increased on addition of silica fillers [Figure 4(b), Table II]. A decrease of supercooling, $\Delta T = T_m - T_c$, is related to ability of filler particles to promote heterogeneous nucleation in the iPP matrix.[14,25] Silica particles with polar surfaces (microsilica S-120 with hydroxyl groups and nanosilica A-R7200 with methacryl layers) produced greater T_c shifts, less supercooling and stronger nucleation effect in the iPP matrix. Regarding the size of unmodified silica fillers, nucleation effect of nanosilica A-200 was somewhat weaker than of microsilica S-120.

Morphology of the iPP/Silica Composites

The influence of size and properties of silica particles on the spherullite size of iPP matrix was studied. SEM micrographs of the iPP microsilica 92/8 composites reveal few micro-sized silica particles at fractured surfaces [Figure 5(a)]. Lower number of hollows from which microsilica particles were pulled out at the etched surface of the iPP/S-D17 than iPP/S-120 composite might indicate better compatibility of the iPP matrix with nonpolar S-D17 compared to polar S-120 particles. SEM micrographs of fractured iPP/nanosilicas [represented by iPP/A-200 and iPP/A-R8200 92/8 composites in Figure 5(b)] reveal relatively homogeneous distribution of nanosilica particles and agglomerates. Micrographs in Figure 5(b) also reveal more homogeneous dispersion and lower degree of agglomeration of modified nonpolar A-R8200 than hydrophilic A-200 nanosilica. Higher amount of nanosilicas than microsilicas in SEM micrographs of fractured surfaces indicates better interactivity of the iPP matrix with nanosized silica particles than with microsized silica particles.

Fillers might affect nucleation, microstructure, crystallization rate, transcrystallinity, orientation, and crystallite and spherulite size in a polymer matrix.[2,3] The most pronounced effect of the silica filler in iPP/silica composites is on the iPP spherulite size (diameter, d_{sph} in Figure 6). The effect of the particle properties (size, shape, and surface treatment) on the spherulite growth rate and size under isothermal and nonisothermal crystallization conditions were observed by different authors.[15–18,26,27] Through the whole concentration range of added silica fillers following changes of the spherulite size could be recognized: (1) decrease of spherulite size up to 2 vol %, (2) plateaus in the concentration range 2–6 vol %, and (3) second decrease with tendency to equal values of spherulite size at 8 vol % of added silica.

Abrupt decrease in spherulite size with the lowest silica addition (up to 2%) can be ascribed to the strong nucleation effect.[2–5,20] Filler particles could act as heterogeneous nuclei, thus increasing the total number of nuclei and leading to a larger number of smaller spherulites. Addition of silicas with polar surfaces (S-120, A-200, and A-R7200) caused higher crystallization temperature and affected nucleation stronger than modified nonpolar silicas (S-D17 and A-R8200). The levels of two plateaus at the intermediate silica concentration (2–6 vol %) seem to be initially determined by the different nucleation ability of various silica grades observed at 2 vol % of added silica. Accordingly, silicas with modified nonpolar surfaces (S-D17 and A-R8200) exhibit higher spherulite size than silicas with polar surfaces (S-120, A-200, and A-R7200) in whole concentration range. The shape of all silica particles could not cause such differences in spherulite size because there are no tubular silica species with stronger nucleation effect than spherical silica particles.[18] The fact, that spherulite size is stronger affected by character of silica

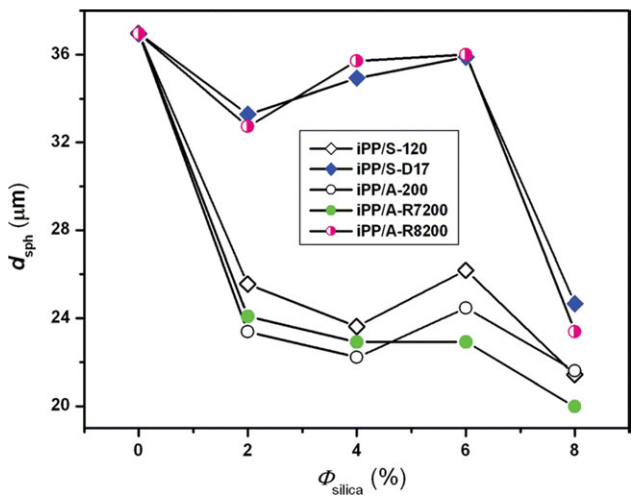

Figure 6. Average spherulite diameter, d_{sph}, of iPP/silica composites vs. volume fraction of added silica (ϕ_{silica}) determined from POM micrographs. [Color figure can be viewed in the online issue, which is available at wileyonlinelibrary.com.]

Applied Polymer SCIENCE

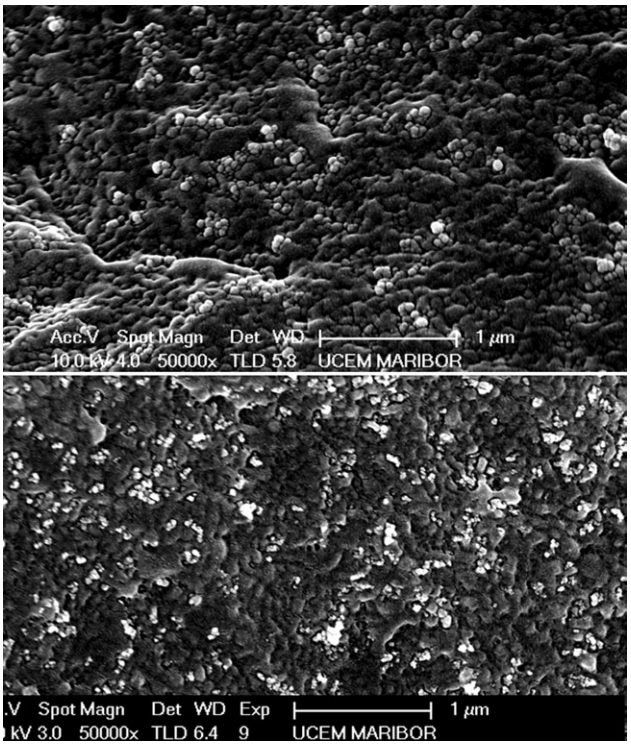

Figure 7. SEM micrographs of iPP composites with 4 vol % of nanosilica A-R7200 (top) and A-R8200 (bottom) fillers.

filler surfaces than by silica particle size (micro vs. nano) was unexpected, but explainable. Ray et al.[26] proved lower primary average nucleation density of the crystallites in poly[(butylene succinate)-*co*-adipate] (PBSA) nanocomposite with filler cloisite*30B which is more miscible with PBSA matrix than with cloisite*20A. Authors also proposed, that secondary nucleation in nonisothermal crystallization of the PBSA/C30B nanocomposite is not active what led to significantly enlarged spherulites. Wang et al.[27] also concluded that spherulite growth rate of the isothermally crystallized polypropylene matrix is influenced by interfacial adhesion that was altered by surface treatment of the $BaSO_4$ filler. They also proposed that retardations of polymer chains movement by particle–matrix interaction may decrease spherulite growth rate additionally.[27] According to above explanation[26,27] nonpolar silicas might nucleate lower number of the crystallites than polar silicas during primary and secondary crystallization. Therefore, considerably larger spherulite arose in the iPP matrix with more miscible nonpolar S-D17 and A-R8200 silicas than with hydrophylic silicas (S-120 and A-200) and methacrylsilanized A-R7200 nanosilica.

Analysis of SEM and OM/POM micrographs of the iPP/silica 96/4 composites (typical of the middle concentration range from 2 to 6 vol %) confirmed intraspherulitic accommodation of nanosilica particles ($d_p = 12$ nm) and agglomerates ($d_p \sim 100$ nm) besides of their interspherulitic locations. Separated dark areas without nanosilica particles and areas with white nanosilica spots in SEM micrographs represented by Figure 5(b) indicate preferential accommodation of the nanosilica particles/aggregates within some regions. SEM micrographs in Figure 7 suggest accommodation of nanosilica particles and agglomerates within holes. Schematic presentation in Figure 8, constructed on the basis of the polyethylene TEM micrograph from the paper of Keith et al.,[28] illustrated suitable accomodation of nanosilica agglomerates (up to ~100 nm) between interlamellar links without distortions. Despite of their preferential allocation in less ordered regions [white spots areas in Figure 5(b)], the dispersion looks relatively homogeneous (Figure 8). Such illustration suggests the possibility of undisturbed spherulite growth and application of structural models like cluster model[15] to iPP/nanosilica composites. Because there is no argument was found in literature for a modified morphology around nanoparticles,[3] it might be supposed that filler particles became embedded into growing spherulite and were not ejected by the forces in the crystallizing material. The study of Karger-Kocsis et al.[29] of analogous polypropylene blends, which revealed intraspherulitically and interspherulitically disperded particles of propylene-based copolymers, might support this conclusion. Namely, intraspherulitically dispersed EPDM particles did not influence radial spherulite growth despite of their relatively high average size (~1 μm). The spherulites grew until dispersed particle surface became encompassed and then continued to grow further without modifying radial lamellar growth.[29] Lipatov[30] also proposed that filler particles up to 1 μm in particulated polymer composites may be fully situated in the disordered interstructural regions.

Well-developed spherulites in the iPP composites with relatively high microsilica S-D17 contents (4 and 6 vol %, Figure 6) is an astonishing result. Smaller nano-sized silica particles in these composites could be accommodated intra- and interspherulitically as POM and SEM micrographs suggested (not shown). POM micrograph (left) and its schematic presentation (right) in Figure 9 revealed prevalent interspherulitic accommodation of micro-sized silica particles in the composite with 4 vol % of S-D17 (Figure 9). Obviously, silica microparticles (10 μm) could not be engulfed by spherulites like filler and elastomer particles

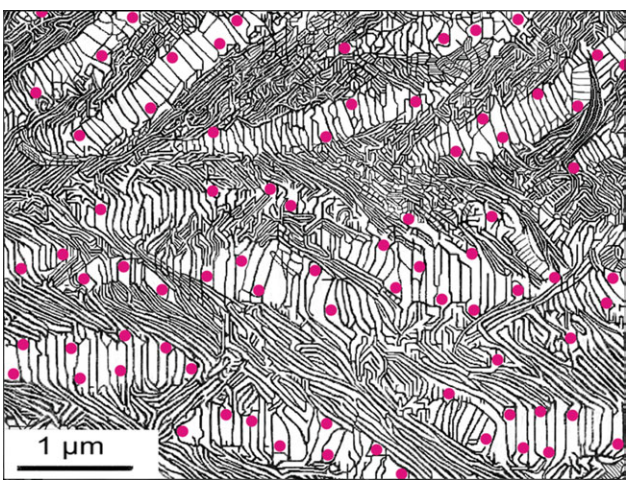

Figure 8. Schematic presentation of the nanosilica agglomerates (full circles ~100 nm) accommodated into low ordered interlamellar regions. [Color figure can be viewed in the online issue, which is available at wileyonlinelibrary.com.]

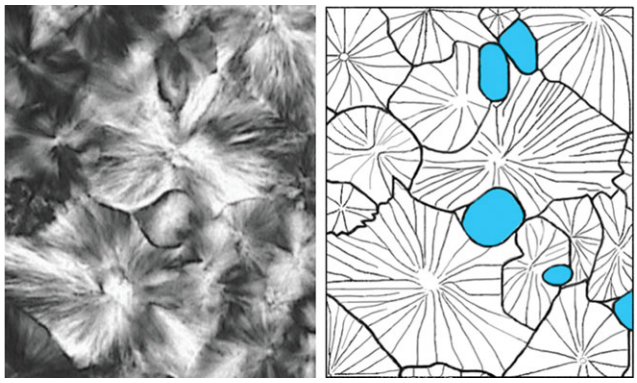

Figure 9. POM micrograph of the iPP/S-D17 96/4 composite (left) and its schematic presentation (right). [Color figure can be viewed in the online issue, which is available at wileyonlinelibrary.com.]

up to 1 μm. OM/POM micrographs in Figure 10 illustrate suitable interspherulitic allocations of the microsized S-D17 particles that do not obstruct the growth of large spherulites even in the iPP composite with 6 vol % of S-D17. However, interspherulitic accommodation of microsized silica particles could not explain are these microparticles ejected to the spherulite surfaces or they stopped the spherulite growth regardless of their nucleation ability.[3,30–33]

A second pronounced decrease in spherulite size occurred at 8 vol % of silica (third concentration range in Figure 6) implies either diminishing effect of factor(s) favorable for the spherulite growth, or some new effect is superposed to the nucleation effect. Abrupt decrease with tendency to equal the values of spherulite size at 8 vol % of added silica in Figure 6 confirm that the influence of filler (size, surface modification) on the size and growth rate of reduced spherulite size could be explained by lamellar clustering crystallization process and by

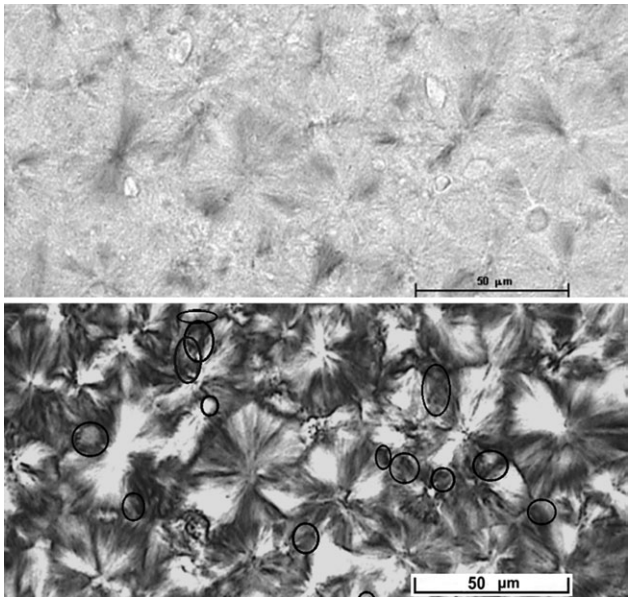

Figure 10. OM (top) and POM (bottom) micrographs of the iPP/S-D17 94/6 composite with accommodated microparticles surrounded by circles.

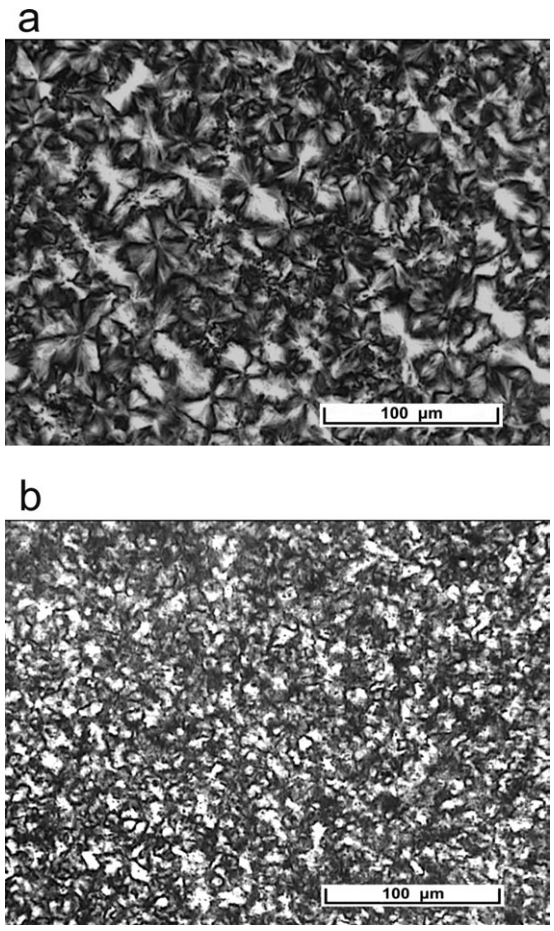

Figure 11. POM micrographs of the iPP/silica 98/2 composite with (a) hydrophobic S-D17 microsilica and (b) polar A-R7200 nanosilica.

restricted diffusive mobility of polymer chains due to the presence of silica nanoparticles.[14–18] Moreover, restrained spherulite growth in composites with microsilicas could be also explained by topological or spatial constraints caused by inorganic fillers, that promote spherulites to reach sizes comparable to the distance between filler particles.[32,33]

However, regular spherulites still persist in the composites containing silica fillers with nonpolar surfaces (S-D17 and A-R8200) despite possible restraining steric hindrances of fillers [Figure 11(a)]. In composites with polar silica surfaces (S-120, A-200, and A-R7200), the morphology with thin, dark branched spherulitic grains without Maltese crosses prevails, especially in composites with methacrylsilanized A-R7200 [Figure 11(b)]. This transformation of spherulites confirms the conclusion that polymers containing high filler concentration crystallize to a loose spherulite structure.[30]

CONCLUSIONS

Microsilica particles and their agglomerates were relatively homogeneously incorporated into the iPP matrix and influenced final supermolecular structure rather than the phase structure of iPP/silica composites. Structural characteristics (phase structure, crystallite size, crystallite orientation, crystallinity) were almost

unaffected by incorporation of filler and interactions in the iPP/silica composites were negligible. The addition of all silica grades affected crystallization and decreased spherulite size in the iPP matrix as well as transformed well-developed spherulitic morphology to the morphology with irregular spherulitic grains. Altough filler particle size played important role in spherulite growth, surface modification of considered silica fillers exhibited stronger influence on spherulite size than size of silica particles. Filler particles S-D17 and A-R8200 with nonpolar surfaces enabled better spherulitic growth than polar S-120, A-200, and A-R7200 filler particles. Accordingly, nucleation ability of nonpolar silicas is supposed to be lower since they are more miscible/compatible with iPP chains than silicas with polar surfaces. Suitable interspherulitical accommodations of the micro-sized S-D17 particles enable growth of well developed spherulites even in the iPP composite with 6 vol % of the S-D17. Almost equal values of spherulite sizes at 8 vol % of silicas confirmed the conclusion that the size and growth rate of the spherulites becomes insignificant above optimum filler concentration and independent of the surface modification.

ACKNOWLEDGMENTS

Financial support of the Ministry of Science, Education and Sports of the Republic of Croatia (Grant No. 098-0982904-2955) and the Ministry of Higher Education, Science and Technology of the Republic of Slovenia is acknowledged. The authors are most grateful to Dr. Uwe Schachtely for his advice concerning the choice of nano- and microsilicas as well as Degussa AG for generous donation of silica samples.

REFERENCES

1. Wagner, M. P. In Additives for Plastics; Seymour, R. B., Ed.; Academic Press: New York, **1978;** Vol. *1*, p 9.
2. Rothon, R. N. Particulate-Filled Polymer Composites, 2nd ed. Rapra: Shawbury, **2006;** Chapter 8, p 357.
3. Wypych, G. Handbook of Fillers, 2nd ed.; ChemTec Publishing: Toronto, **2000;** Chapters 10 and 15.
4. Pukanszky, B. In Handbook of Polyolefins, 2nd ed.; Vasile, C., Ed.; Marcel Dekker: New York, **2000;** p 689.
5. Šmit, I.; Denac, M.; Švab, I.; Radonjič, G.; Musil, V.; Jurkin, T.; Pustak, A. *Polimeri* **2009,** *30*, 183.
6. Garcia, M.; Van Vliet, G.; Jain, S.; Schrauwen, A. G.; Sarkissov, A.; van Zyl, W. E.; Boukamp, B. *Rev. Adv. Mater. Sci.* **2004,** *6*, 169.
7. Rong, M. Z.; Zhang, M. Q.; Pan, S. L.; Friedrich, K. *J. Appl. Polym. Sci.* **2004,** *92*, 1771.
8. Wu, C. L.; Zhang, M. Q.; Rong, M. Z.; Friedrich, K. *Compos. Sci. Technol.* **2002,** *62*, 1327.
9. Cai, L. F.; Huang, X. B.; Rong, M. Z.; Ruan, W. H.; Zhang, M. Q. *Polymer* **2006,** *47*, 7043.
10. Zhou, T. H.; Ruan, W. H.; Mai, Y. L.; Rong, M. Z.; Zhang, M. Q. *Compos. Sci. Technol.* **2008,** *68*, 2858.
11. Bikiaris, D. N.; Papageorgiou, G. Z.; Pavlidou, E.; Vouroutzis, N.; Palatzoglou, P.; Karayannidis, G. P. *J. Appl. Polym. Sci.* **2006,** *100*, 2684.
12. Papageorgiou, G. Z.; Achilias, D. S.; Bikiaris, D. N.; Karayannidis, G. P. *Thermochim. Acta* **2005,** *427*, 117.
13. Jain, S.; Goossens, H.; van Duin, M.; Lemstra, P. *Polymer* **2005,** *46*, 8805.
14. Asuka, K.; Liu, B.; Terano, M.; Nitta, K. *Macromol. Rapid Commun.* **2006,** *27*, 910.
15. Nitta, K.; Asuka, K.; Liu, B.; Terano, M. *Polymer* **2006,** *47*, 6457.
16. Waddon, A. J.; Petrovic, Z. S. *Polym. J.* **2002,** *34*, 876.
17. Xu, J. T.; Zhao, Y. Q.; Wang, Q.; Fan, Z. Q. *Polymer* **2005,** *46*, 11978.
18. Palza, H.; Vera, J.; Wilhelm, M.; Zapata, P. *Macromol. Mater. Eng.* **2011,** *296*, 744.
19. Pustak, A.; Leskovac, M.; Denac, M.; Švab, I.; Pohleven, J.; Makarovič, M.; Musil, V.; Šmit, I. Submitted to publication.
20. Pukanszky, B.; Belina, K.; Rockenbauer, A.; Maurer, F. H. J. *Compos. A* **1994,** *25*, 205.
21. Alexander, L. E. X-Ray Diffraction Methods in Polymer Science; Wiley: New York, **1969;** p 138.
22. Zipper, P.; Janosi, A.; Wrentschur, E. *J. Phys. IV Suppl. J. Phys. I* **1993,** *3*, 33.
23. Painter, P. C.; Watzek, M.; Koenig, J. L. *Polymer* **1977,** *18*, 1169.
24. Vijayalakshmi, U.; Balamurugan, A.; Rajeswari, S. *Trends Biomater Artif Organs* **2005,** *18*, 101.
25. Lonkar, S. P.; Morlat-Therias, S.; Caperaa, N.; Leroux, F.; Gardette, J. L.; Singh, R. P. *Polymer* **2009,** *50*, 1505.
26. Ray, S. S.; Bandyopadhyay, J.; Bousmina, M. *Eur. Polym. J.* **2008,** *44*, 3133.
27. Wang, K.; Wu, J. S.; Zeng, H. *Eur. Polym. J.* **2003,** *39*, 1647.
28. Keith, H. D.; Padden, F. J.; Vadimsky, R. G. *J. Polym. Sci. A2* **1966,** *4*, 267.
29. Karger-Kocsis, J.; Kiss, L.; Kuleznev, V. N. *Polym. Commun.* **1984,** *25*, 122.
30. Lipatov, Y. S. Polymer Reinforcement; ChemTec Publishing: Toronto-Scarborough, **1995;** Chapter 4, p 153.
31. Singhal, A.; Fina, L. J. *Polymer* **1996,** *37*, 2335.
32. Burke, M.; Young, R. J.; Stanford, J. L. *Plast. Rubber Process Appl.* **1993,** *20*, 121.
33. Manias, E.; Polizos, G.; Nakajima, H.; Heidecker, M. J. In Flame Retardant Polymer Nanocomposites; Wilkie, C., Ed.; Hoboken: New York, **2007;** p 31.